Rheol Acta (2011) 50:107–115
DOI 10.1007/s00397-010-0524-z

ORIGINAL CONTRIBUTION

Hysteresis cycles and fatigue criteria using anelastic models based on fractional derivatives

Michele Caputo · José M. Carcione

Received: 30 January 2010 / Revised: 25 July 2010 / Accepted: 23 December 2010 / Published online: 12 January 2011

Abstract The constitutive equation and the fatigue of anelastic media are described by using fractional order derivatives. The stress–strain relation, based on a generalization of the Kelvin–Voigt model, describes typical hysteresis cycles with the stress increasing as the number of cycles increases, a phenomenon known as cyclic hardening and observed in many materials such as, for instance, steel. Criteria are established to find the number of cycles which may cause fatigue for a strain with a given amplitude and frequency. They are based on the yield and fatigue stresses, on the melting temperature through the dissipated energy, and on the strain energy. In all the cases, it is seen that the number of cycles to failure is inversely proportional to the amplitude and to the frequency of the applied strain. Comparison to experimental data indicates that the model satisfies, at least qualitatively, the behavior of real materials under cyclic loading.

Keywords Anelasticity · Fractional derivatives · Hysteresis · Fatigue

Introduction

In many applications, materials are subjected to vibrations or oscillatory forces. The behavior of materials under such conditions differs from that of static loads, where the failure criteria to use are based on the static yield stress. The fatigue stress due to cyclic loading is generally smaller than the yield stress. There are many factors that affect fatigue life, namely the nature of the cyclic stress, the geometry of the medium, the type of material, the presence of residual stresses and internal defects, the grain size, the temperature, etc. (Ellyin 1996; Lee et al. 2004). The process can be summarized in three stages: crack initiation, crack propagation, and ultimate ductile failure. These are complex phenomena which require the collection of much experimental data and appropriate constitutive equations.

Since long time, mathematics and physics have given attention to the modeling of the dissipation and dispersion of waves, of the propagation of energy in solid anelastic media, in plasmas, in fluids, and in solid dielectrics. The introduction of the first-order derivatives in the constitutive equations of elasticity, leading to the so-called Kelvin–Voigt, Maxwell and standard linear solid (or Zener) models, or the introduction of derivatives of higher order, was, in some cases, unsuccessful in explaining the decay of energy and the dispersion (Caputo 1967).

Heaviside (1894), with his symbolic calculus, studied the propagation of electromagnetic energy, Cisotti (1911) introduced memory formalisms to represent dispersion and dissipation, and Graffi (1928) and Cole and Cole (1941) studied induced polarization assuming a frequency-dependent complex dielectric parameter. The study of the dissipation of elastic energy is fundamental in the work of Bagley and Torvik (1986), who assumed a frequency-dependent relation between stress and strain based on fractional derivatives. The use of derivatives of real-order q is now becoming more

M. Caputo
Department of Physics, University "La Sapienza",
Rome, Italy

J. M. Carcione (✉)
Istituto Nazionale di Oceanografia e di Geofisica
Sperimentale (OGS), Borgo Grotta Gigante 42c,
34010 Sgonico, Trieste, Italy
e-mail: jcarcione@inogs.it

popular in applied physics, especially in the formulation of the constitutive equations of dispersive media and the description of diffusive phenomena. In fact, from problems of dissipation of energy in anelastic media (Caputo 1967; Caputo and Mainardi 1971), the use of fractional derivatives has been extended to the study of the rheology of the Earth (Körnig and Müller 1989), to seismic prospecting (Carcione et al. 2002; Carcione 2009), to diffusion matters (Mainardi and Pagnini 2003; Wyss 1986), to problems of electric energy storage (Jacquelin 1991), to geoelectric prospecting (Caputo and Plastino 1998; Weiss and Everett 2007), to medicine (Craiem and Armentano 2007), and to the dispersion and attenuation of electromagnetic waves in plasmas and in fluid media (Caputo 1995a, b).

We propose a simple constitutive equation, based on fractional derivatives, that generalizes Hooke's law and the Kelvin–Voigt model. The stress is analyzed for a periodic saw-tooth strain function, showing that hysteresis is a consequence of the fractional derivative. The hysteresis cycle implies a stress increase as the number of cycles increases. This is one of the mechanisms to bring the material to failure. Moreover, fatigue due to energy considerations is also investigated.

The stress–strain relation

Caputo (1979) described the anelastic behavior of many materials over wide frequency ranges by using fractional derivatives. The corresponding constitutive stress (τ)–strain (ϵ) relation for a given deformation is

$$\tau = \mu\epsilon + \eta\frac{\partial^q \epsilon}{\partial t^q}, \quad 0 < q < 1, \tag{1}$$

where μ and η are the stiffness and a pseudo-stiffness, respectively. In the case of shear deformations, μ and η are the rigidity modulus and the pseudo-viscosity; η is a shear stiffness for $q = 0$ and a viscosity for $q = 1$. In general, the interpretation of these parameters depends on the type of deformation. The limits $q = 0$ and $q = 1$ in the second term of the right-hand side of Eq. 1 give Hooke's law and the constitutive relation of a dashpot. The last case is the Kelvin–Voigt model (Carcione 2007).

In the frequency domain, we obtain

$$\tau = \bar{\mu}\epsilon, \tag{2}$$

where

$$\bar{\mu} = \mu + (\mathrm{i}\omega)^q \eta \tag{3}$$

is the complex stiffness, with $\mathrm{i} = \sqrt{-1}$ and ω the angular frequency. Since q is a rational number, there may be more than one mathematical solution. We consider the first Riemann sheet.

Equation 1 was generalized by Caputo and Mainardi (1971) as

$$\left(\alpha + \beta\frac{\partial^q}{\partial t^q}\right)\tau = \left(\mu + \eta\frac{\partial^q}{\partial t^q}\right)\epsilon, \tag{4}$$

where α and β are parameters with the appropriate dimensions. In this case,

$$\bar{\mu} = \frac{\mu + (\mathrm{i}\omega)^q \eta}{\alpha + (\mathrm{i}\omega)^q \beta}. \tag{5}$$

This is the generalized Zener model in elasticity or the Cole–Cole model in electromagnetism (Cole and Cole 1941; Carcione 2007). Bagley and Torvik (1986) have shown that relations 1 and 4 are causal and represent the decay of the energy of the vibrations and, in general, the anelastic properties of a wide class of anelastic media. In particular, the relation 1 was proposed to represent the phenomenon of fatigue of anelastic materials (Caputo 1979).

The phenomenological model of fatigue

To see how Eq. 1 leads to fatigue, let us consider an input signal $\epsilon(t)$ with the form of the periodic saw tooth, with period $4a$ and amplitude ϵ_0 shown in Fig. 1. This type of deformation is preferred to the sinusoidal variation because it allows us to see the deviations from the linear behavior.

The derivative of real order is defined as follows (Podlubny 1999; Mainardi 2010; Diethelm 2010):

$$\frac{\partial^q \epsilon(t)}{\partial t^q} = \frac{1}{\Gamma(1-q)}\int_0^t (t-\xi)^{-q}\epsilon'(\xi)d\xi, \quad 0 < q < 1, \tag{6}$$

where the prime denotes the first derivative and Γ is the gamma function. We have $\epsilon' = (-1)^r \epsilon_0/a$, where

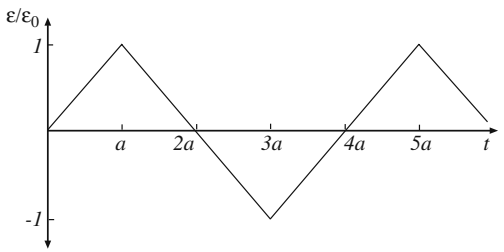

Fig. 1 Strain applied for the estimation of the hysteresis cycle

Table 1 Analytic expression of the first two loops of the hysteresis cycle, where $p = 1 - q$

	r	ϵ/ϵ_0	t/a	$ap!(d^q\epsilon/dt^q)/\epsilon_0$
$n = 0$	0	0, 1	0, 1	t^p
	1	1, −1	1, 3	$t^p - 2(t-a)^p$
$n = 1$	2	−1, 1	3, 5	$t^p - 2(t-a)^p + 2(t-3a)^p$
	3	1, −1	5, 7	$t^p - 2(t-a)^p + 2(t-3a)^p - 2(t-5a)^p$
	4	−1, 1	7, 9	$t^p - 2(t-a)^p + 2(t-3a)^p - 2(t-5a)^p + 2(t-7a)^p$

$2r - 1 < t/a < 2r + 1$. Then, from Eqs. 1 and 6, the stress response of the medium for this time interval is

$$\tau = \mu\epsilon(t) + \frac{\eta\epsilon_0}{a(1-q)!}\left[t^{1-q} + 2\sum_{j=1}^{r}(-1)^j(t - 2ja + a)^{1-q}\right], \tag{7}$$

where we have used the property $(1 - q)\Gamma(1 - q) = (1 - q)!$.

Ignoring for the moment the first term of the right-hand member of Eq. 7, which gives no contribution to anelastic phenomena, the analytic expression of Eq. 7 for the first two and half cycles is specified in Table 1 and represented in Fig. 2. We may see that the loop does not repeat itself exactly. This means that an increasing stress is needed to produce successive deformations $+\epsilon_0$ or $-\epsilon_0$, but the successive increases converge to zero. For $q = 0$, obviously there is no hysteresis. For instance, let us consider the stress increment shown in Fig. 2 for $n = 0$, i.e., $\tau(t = 5a) - \tau(t = a)$. We obtain $[\eta\epsilon_0/(a^q(1 - q)!][5^p - 2(4^p) + 2(2^p) - 1]$, where $p = 1 - q$. The increase in τ when the hysteresis loop goes from the n-th cycle to the $n + 1$-th cycle is

$$\delta(n) = \tau_0 g(n, 1 - q), \quad \tau_0 = \frac{\eta\epsilon_0}{a^q(1 - q)!} \tag{8}$$

where

$$g(x, p) = (4x + 5)^p - 2(4x + 4)^p + 2(4x + 2)^p - (4x + 1)^p \tag{9}$$

Note that $\delta(n) = 0$ for $q = 1$. The total increase after N cycles is

$$\Delta\tau(N) = \sum_{n=0}^{N}\delta(n), \tag{10}$$

which is positive and limited for $0 < q < 1$. The curves in Fig. 2 agree with the process of transient cyclic hardening typically observed in most materials (e.g., Figure 5.8 in Lee et al. 2004).

We see from Eq. 8 that $\Delta\tau(N)$ increases with ϵ_0 and with decreasing a (high frequencies). Figure 3 shows the stress increase as a function of N for $q = 0.1$, 0.3, and 0.5. We observe that $\Delta\tau$ is maximum for $n = 0$ and then decreases very rapidly. This is in agreement with experimental data (Rao 1995; Zhuang and Halford 2001). As a result, the first stress increases are the most significant and $N = 5$ gives a good estimate of $\Delta\tau(\infty)$. Moreover, the $\Delta\tau$ increases with q, but there is a limit. In fact, the maximum stress increases, $\Delta\tau(\infty)$, as a function of q is shown in Fig. 4, where the maximum value occurs for $q = 0.45$.

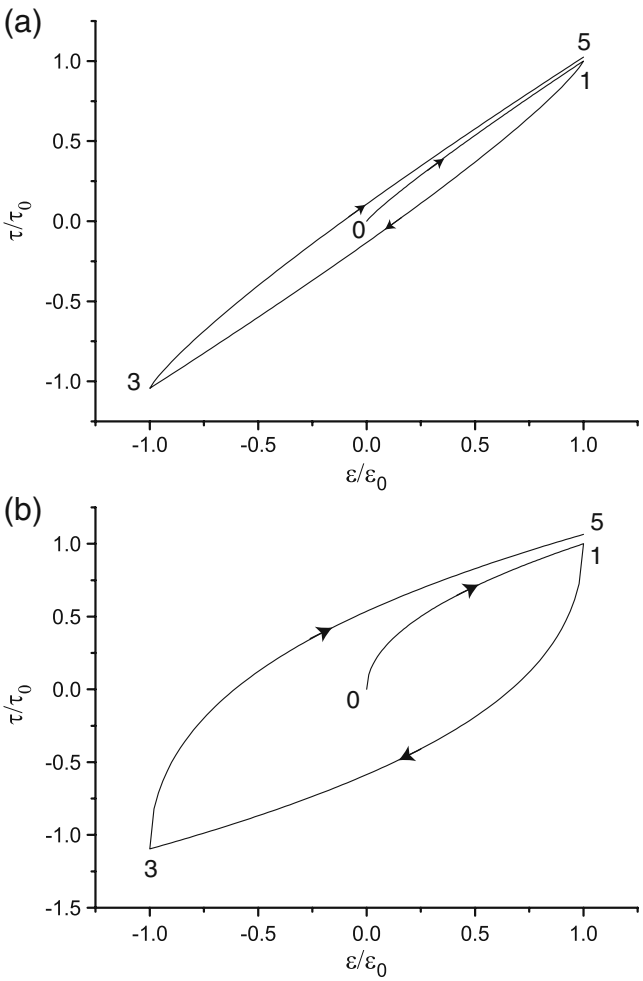

Fig. 2 Hysteresis loop for $q = 0.1$ (**a**) and $q = 0.5$ (**b**), where $\tau_0 = \eta\epsilon_0/[a^q(1 - q)!]$

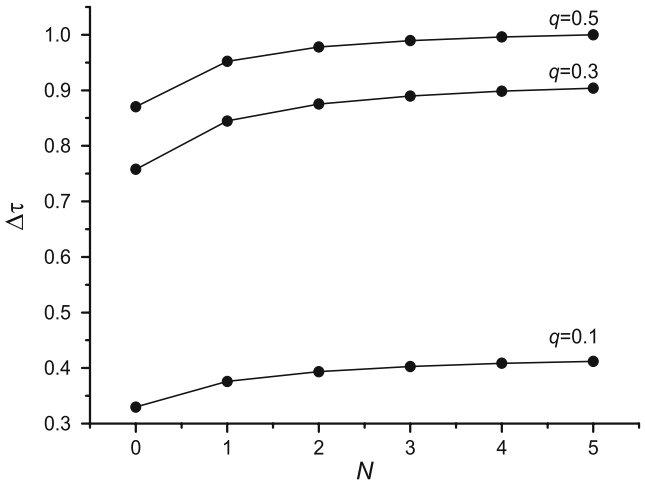

Fig. 3 Total stress increase as a function of the number of cycles, normalized with respect to $\Delta\tau(N=5)$ corresponding to $q=0.5$

The total stress at the cycle N can then be expressed as

$$\tau(N)=\tau(t)=\mu\epsilon(t)+\tau_0+\Delta\tau(N),$$
$$t=(2r+1)a,\quad N=\frac{1}{2}r-1. \tag{11}$$

In terms of N, $t=4Na+5a$ and note that $\epsilon(t)=\epsilon_0$. Then

$$\tau(t)=\bar{\tau}+[\mu+\eta a^{-q}G(N)]\epsilon_0, \tag{12}$$

where

$$(1-q)!G(N)=1+\sum_{n=0}^{N}g(n,1-q) \tag{13}$$

and we have considered a constant stress $\bar{\tau}$ applied to the material in addition to the cyclic one. There is fatigue if the yield stress τ^* lies between $\tau=0$ and $\tau(N=\infty)=\bar{\tau}+[\mu+\eta a^{-q}G(\infty)]\epsilon_0$. Fatigue based on the yield stress is generally achieved before the first cycle, i.e., in the strain interval from $t=0$ to $t=a$ if $\tau^*<\tau(a)=\mu\epsilon_0+\tau_0$, since the stress range (the total stress increase) generated by the hysteresis $\tau(t=\infty)-\tau(t=a)$ is small compared to $\tau(t=\infty)$.

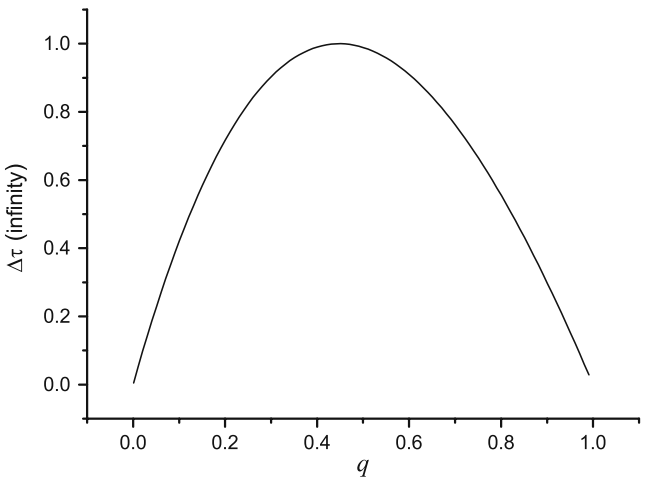

Fig. 4 Normalized maximum stress increase as a function of q

If $\tau^*>\tau(a)$, then fatigue may occur by cyclic loading at a failure time when dislocations and cracks appear in the material. The fatigue stress τ^f due to cyclic loading is lower than the yield stress τ^*. For instance, for alloy steel (39 NiCrMo 3), the yield stress is 1,006 MPa and the fatigue stress is 440 MPa (Biancolini et al. 2006). There is a value N_f of N for which fatigue occurs indicating the limit of the resistance of the material caused by the vibrations. We may obtain explicitly the value of N_f by approximating the function $G(N)$ by the following function:

$$G(N)\approx G_\infty-\left(\phi N^\zeta+\psi\right)^{-1}, \tag{14}$$

where

$$\begin{aligned}&G_\infty=G(\infty),\\&\phi=[G_\infty-G(1)]^{-1}-[G_\infty-G(0)]^{-1},\\&\zeta=(2.438-1.78q)q^{1/3}\\&\psi=[G_\infty-G(0)]^{-1}.\end{aligned} \tag{15}$$

Note that at $n=0$, 1 and ∞, we obtain $G(0)$, $G(1)$, and G_∞, respectively, that ϕ, ζ, and ψ are all positive and $G_\infty-\psi^{-1}>0$. Figure 5 shows the approximation for several values of q. This approximation improves that of Caputo (1979) in his Eq. 4, which corresponds to $G(N)-1$.

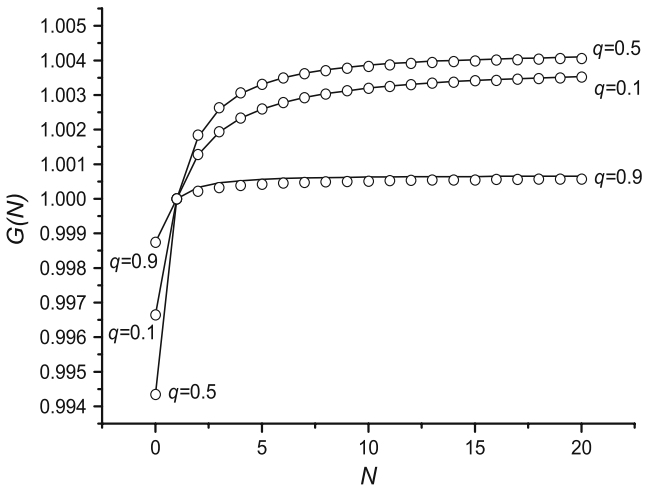

Fig. 5 Approximation (*circles*) of the function $G(n)$ (*solid lines*) by Eq. 15. The curves are normalized by $G(1)$ for a better visualization

Table 2 Fatigue test data for 18 Cr-10Ni-Ti steel (Material BIV) (Yoshida et al. 2001)

T (°C)	ϵ_0	$a(s)$	N_f
20	0.03	2.24	628
	0.02	1.5	1,561
	0.01	0.75	6,229
	0.007	0.52	13,410
450	0.03	2.24	248
	0.02	1.5	1,277
	0.01	0.75	5,347
	0.006	0.45	14,665
600	0.03	2.24	195
	0.02	1.5	542
	0.01	0.75	2,914
	0.006	0.45	8,447
750	0.02	1.5	345
	0.014	1.07	779
	0.01	0.75	1,298
	0.006	0.45	4,410

Substituting Eq. 15 into Eq. 12 and assuming that fatigue occurs at the stress $\tau^f < \tau^*$ gives

$$\tau^f = \bar{\tau} + \left\{\mu + \eta a^{-q}\left[G_\infty - \left(N_f{}^{\zeta}\phi + \psi\right)^{-1}\right]\right\}\epsilon_0. \quad (16)$$

Then

$$N_f = \left\{\left[G_\infty - \frac{a^q}{\eta}\left(\frac{\tau^f - \bar{\tau}}{\epsilon_0} - \mu\right)\right]^{-1} - \psi\right\}^{1/\zeta} \phi^{-1/\zeta}. \quad (17)$$

Yoshida et al. (2001) provide experimental data for metals (see Table 2). One may notice that the number of cycles to failure is decreasing with the strain. The data are represented in Fig. 6, as N_f as a function of the strain. The plots indicate that N_f is a decreasing function of ϵ_0, in agreement with our model.

Fatigue criteria

Yield stress

We may assume, in agreement with experimental data, that the yield stress τ^*, corresponding to N^*, be a decreasing function of the temperature T. Fatigue occurs when

$$\tau^* = k(T' - T), \quad T < T', \quad (18)$$

where T' is the temperature at which the material, with the applied stress, has nil elastic reaction to traction or to bending at the frequency under examination and k is a constant depending on the material (e.g., *Characterization and Failure Analysis of Plastics*, published by ASM International, p. 201).

Another criterion to estimate when fatigue will occur may be based on the result that laboratory experiments on many rocks have indicated that their failure occurs when the applied stress is $\tau^* = \gamma\mu$, where γ ranges from 0.03 to 0.13 with an average of 0.076 and μ is assumed to be the shear modulus (e.g., *Characterization and Failure Analysis of Plastics*, published by ASM International, p. 201).

Energy

The Umov–Poynting theorem or energy balance equation for harmonic fields in anelastic media is given by

$$\mathrm{div}\cdot\mathbf{p} - \mathrm{i}\omega(S - K) + D = 0 \quad (19)$$

(e.g., Carcione 2007, Eq. 4.57), where $\mathbf{p}$ is the power-flux vector, S is the strain (stored) energy, K is the kinetic energy, and D is the dissipated energy. These are energy densities, i.e., time-averaged energies in one cycle per unit volume.

Dissipated energy criterion

The time-averaged dissipated energy density per cycle is given by

$$D = \frac{1}{2}\mathrm{Im}(\bar{\mu})|\epsilon|^2 \quad (20)$$

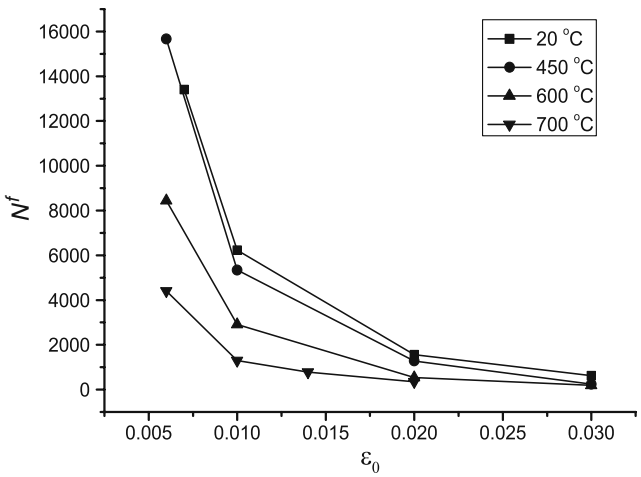

Fig. 6 Number of cycles to failure as a function of the strain amplitude and temperature

(see Eqs. 2.105, 4.85, and 4.114 in Carcione 2007), where Im(·) denotes imaginary part. For $\epsilon = \epsilon_0 \exp(\mathrm{i}\omega t)$, we have

$$D = \frac{1}{2}\epsilon_0^2 \eta \omega^q \sin\left(\frac{\pi q}{2}\right). \tag{21}$$

The amount of dissipated heat in N cycles is equal to the volumetric heat capacity c times the temperature change. Assuming an initial temperature T_0, we have

$$N^m D = Vc(T_m - T_0), \tag{22}$$

where N_m is the number of cycles to reach melting, T_m is the melting temperature, and $V = 1$ is the (unit) volume. Combining the last two equations yields

$$N_m = \frac{2c(T_m - T_0)}{\epsilon_0^2 \eta \omega^q \sin(\pi q/2)}. \tag{23}$$

As can be seen, N_m decreases with increasing frequency and amplitude of the oscillations, while increases with the melting temperature, as expected. Moreover, N_m increases for decreasing q. Actually, the number of cycles to reach the fatigue stress is generally much less than N_m ($N_f \ll N_m$). On the other hand, failure due to the yield stress can be reached at the first cycle if the strain is such that the stress exceeds the yield stress given by Eq. 18.

Equation 23 can be expressed in terms of the quality factor, which is defined as twice the potential energy divided by the dissipated energy (Carcione 2007). This gives $Q = \mathrm{Re}(v^2)/\mathrm{Im}(v^2)$, where $v^2 = \bar{\mu}/\rho = [\mu + \eta(\mathrm{i}\omega)^q]/\rho$, where v is the complex velocity, ρ is the mass density, and Re and Im take real and imaginary parts, respectively. An alternative definition considers the total energy instead of twice the potential energy (see Eq. 3.1.30 in Carcione 2007). In this case, $Q = \mathrm{Re}(v)/[2\ \mathrm{Im}(v)]$. The two quality factors have similar values for $Q \gg 1$. Using the first definition, we obtain

$$Q = \frac{\mu + \omega^q \eta \cos(\pi q/2)}{\omega^q \eta \sin(\pi q/2)}. \tag{24}$$

Then

$$N_m = \frac{2c(T_m - T_0)}{\mu \epsilon_0^2}\left[Q - \cot\left(\frac{\pi q}{2}\right)\right]. \tag{25}$$

Note that N_m increases with Q, as expected, since low Q is generally an indication of a weak material. If q is less but close to 1, $Q \gg 1$ and $N_m \approx 2c(T_m - T_0)Q/(\mu\epsilon_0^2)$. In principle, if one knows Q at a given frequency, it is possible to obtain η from Eq. 24. When dealing with fractional derivatives, such as that of Eq. 1, the material parameters have no standard units. To clarify this issue, a dimensional analysis of the preceding equations in the MKS system follows.

$\tau, \mu \rightarrow$ [Pa = kg/(m s^2)]
$\epsilon \rightarrow$ Dimensionless
$q \rightarrow$ Dimensionless
$\omega \rightarrow$ 1/s
$\eta \rightarrow$ [Pa s^q = kg m^{-1} s^{q-2}]
$D \rightarrow$ [J/m^3 = kg/(m s^2)]
$c \rightarrow$ [J/(m^3 K) = kg/(m s^{2}K)]
$T \rightarrow$ [K]

Note that η has no dimension of dynamic viscosity, unless $q = 1$. This parameter has to be obtained experimentally, for instance, from the quality factor.

Strain energy criterion

The time-averaged strain energy density per cycle is given by

$$S = \frac{1}{4}\mathrm{Re}(\bar{\mu})|\epsilon|^2 \tag{26}$$

(see Eq. 2.104 in Carcione 2007), where Re(·) denotes real part. For $\epsilon = \epsilon_0 \exp(\mathrm{i}\omega t)$, we have

$$S = \frac{1}{4}\epsilon_0^2\left[\mu + \eta\omega^q \cos\left(\frac{\pi q}{2}\right)\right]. \tag{27}$$

The type of failure associated here to the strain energy is a process starting with dislocation movements and the forming persistent slip bands that nucleate short cracks, which is different from failure due to the yield stress (Liu and Ross 1996). Failure occurs when the strain energy in N_f cycles equals a given value S^f:

$$N_f S = S^f. \tag{28}$$

We obtain

$$N_f = \frac{4S^f}{\epsilon_0^2[\mu + \eta\omega^q \cos(\pi q/2)]}. \tag{29}$$

Apparently N_f decreases for increasing stiffness of the material. However, note that S^f should also increase with μ. For instance, Carpick et al. (1997) show that the shear strength of a contact between a silicon nitride tip and muscovite mica depends on the square of the rigidity modulus.

Discussion

The present analysis based on a shear 1D stress–strain relation can equally be applied to the case of compressional and shear deformations using the same mathematical framework. The stress–strain relations for a

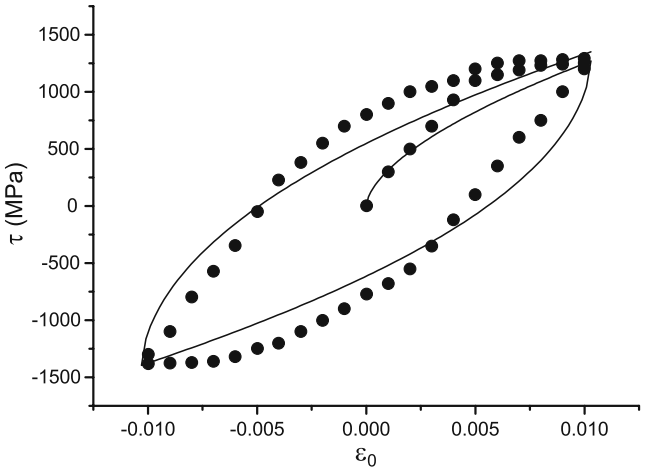

Fig. 7 Hysteresis cycle for $q = 0.4$, $\bar{\tau} = 0$, $\tau_0 = 1{,}270$ MPa, and $\epsilon_0 = 0.0103$ (*solid line*, $\tau - \mu\epsilon_0$) compared to experimental data for aged Inconel 718 at room temperature (*symbols*)

Kelvin–Voigt solid are a simple generalization of those for one-dimensional media (Carcione 2007; Carcione et al. 2004). A further generalization to the fractional-derivative case can be expressed as

$$\sigma_{ij} = \left(\lambda\theta + \lambda' \frac{\partial^p \theta}{\partial t^p}\right)\delta_{ij} + 2\mu\epsilon_{ij} + 2\mu' \frac{\partial^q \epsilon_{ij}}{\partial t^q}, \qquad (30)$$

where λ and μ are the Lamé constants, λ' and μ' are the corresponding anelastic parameters, p and q are the dilatational and shear fractional orders of differentiation, ϵ_{ij} are the strain components (Caputo 1967), $\theta = \epsilon_{ii}$ is the dilatation field, and δ_{ij} is Kronecker's delta. Comparing Eqs. 1 and 30, we see that η corresponds to μ'.

If the cyclic tests are longitudinal, dilatational, or purely shear, Eq. 1 and the present theory adequately describe the failure criteria, since in the first two cases the first term in Eq. 30 describes the stress–strain relation and it is mathematically equivalent to Eq. 1, taking into account that in the longitudinal tests (e.g., pipes, bars, beams) we have to consider the Young modulus of the material. Pure shear tests are described by the second term of Eq. 30.

Shear criteria alone to establish fatigue is, for instance, used by Tao and Xia (2008), who perform strain-range-controlled fully reversed cyclic shearing fatigue tests on thin-walled tubular specimens made of an epoxy polymer. They obtain an empirical relation between the applied strain energy and N_f. Similar cyclic tests can be found in Sugimoto and Sasaki (2008), where typical hysteresis loops of plywood specimens measured at the first loading cycle are shown.

A generalization of the theory presented in this paper to the full 3D case (dilatation and shear) is not the purpose here. This mainly happens in the anisotropic case, where Eq. 30 must be used because all the deformation modes are coupled. The analysis proceeds in the same manner with the difference that more parameters are needed and p and q do not necessarily have the same value. Regarding the criteria based on energy considerations, the equations for the 3D anisotropic (anelastic) case can be found, for instance, in Carcione (2007), since the energy densities can be generalized to the fractional case in the frequency domain by using the correspondence principle. An analysis based on Eq. 30 is more involved from a mathematical point of view (Makris 1997; Carcione 2009) and will be the subject of further research.

Strain hardening is an effect that can be introduced in stress–strain relations based on fractional derivatives. Nicolle et al. (2010) observed that some human tissues get stiffer as shear strain increases. In order to model this behavior, they have introduced a power-law dependence of the strain into the relaxation modulus.

Examples

The ability of the model to describe hysteresis cycles is shown in Fig. 7, where the stress–strain relation ($\tau - \mu\epsilon_0$ versus ϵ) for $q = 0.4$ is compared to experimental data obtained for Inconel 718 superalloy (Zhuang and Halford 2001). It can be seen that the qualitative agreement is good. In this case, the Cole–Cole model represented by Eq. 5 can give a better quantitative fit in view of the additional parameters.

Let us consider, specifically, Inconel 1700–1850F Anneal (www.specialmetals.com). It has a Young modulus $\mu = 200$ GPa at 20°C and 163 GPa at 650°C,

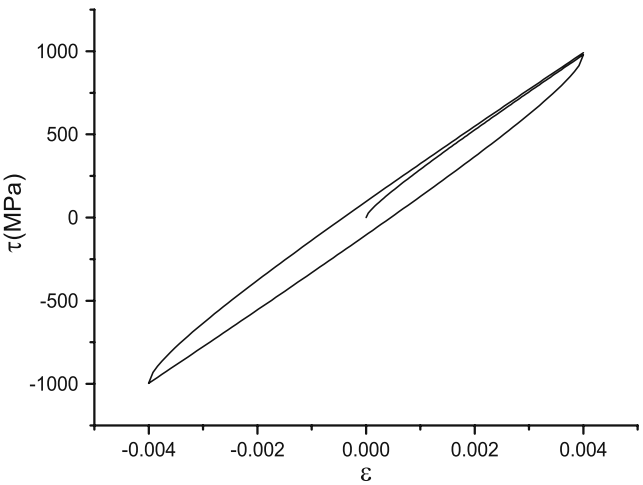

Fig. 8 Hysteresis cycle (τ) for Inconel allow 1700–1850F Anneal, with $q = 0.5$, $\tau_0 = 180.5$ MPa, and $\epsilon_0 = 0.004$

and the yield stress is $\tau^* = 1{,}035$ and 828 MPa. The constant k in Eq. 18 is then $k = 0.17$ MPa/°C and $T' = 6{,}108$°C, although this limit temperature is not realistic since beyond 700°C the dependence is not linear and the yield stress decreases abruptly with temperature. Assuming room temperature, $q = 0.5$, $\eta = 40$ GPa s^q, $a = 1$ s, and $\epsilon_0 = 0.004$, we obtain $\mu\epsilon_0 = 800$ MPa and $\tau_0 = 180.5$ MPa. The stresses at the maxima of the strain ($t = 4Na + 5a$) are $\tau(a) = \mu\epsilon_0 + \tau_0 = 980.5$ MPa, $\tau(5a) = \mu\epsilon_0 + \eta a^{-q} G(0)\epsilon_0 = 992.2$ MPa, $\tau(9a) = \mu\epsilon_0 + \eta a^{-q} G(1)\epsilon_0 = 993.3$ MPa, and $\tau(\infty) = \mu\epsilon_0 + \eta a^{-q} G(\infty)\epsilon_0 = 994.1$ MPa. For instance, for a fatigue stress of $\tau_f = 994.09$ MPa, the number of cycles to failure is $N_f = 2{,}600$. Figure 8 shows the first two cycles of the hysteresis loop, corresponding to the stress $\tau(\epsilon)$ with $\bar{\tau} = 0$.

We now use the dissipated energy criterion for aluminum. Its properties are $\mu = 70$ GPa, $c = 2.4 \times 10^6$ J/(m^3 K), and $T_m = 933$ K. Moreover, we assume a frequency of 3 Hz, i.e., $\omega = 6\pi$/s, $\epsilon_0 = 10^{-4}$, $T_0 = 293$ K, and $q = 0.5$. We obtain η from the quality factor using Eq. 24. For $Q = 1{,}000$, it is $\eta = 22.8$ MPa s^q. Equation 23 gives $N_m = 4.4 \times 10^9$ cycles and $t^m = 1.54$ years to reach melting. However, note that this is the melting time; the failure time t^* can be much smaller.

Finally, consider the strain energy criterion for aluminum and $S^f = 10$ MJ/m^3 (Ellyin 1996). From Eq. 29, the number of cycles to failure is approximately $N_f = 60{,}000$.

Conclusions

We have shown how the introduction of a memory formalism, in particular the derivative of fractional order, in the constitutive equations of anelastic media represents the phenomenon of hysteresis and fatigue. By applying successive strains to the medium, it is seen that the stress increases when the strain assumes repeatedly the same value. The model then describes the process of cyclic hardening, where the stress developed in each successive strain reversal increases as the number of cycles increases. The rate of change of the applied stress will gradually reduce in the first few cycles to reach a stable level (a steady-state condition) and remain stable till fatigue occurs due to the appearance of the first fatigue crack.

If the stress becomes larger than a threshold typical of the medium, then failure occurs. If this stress is the yield stress, then fatigue mainly occurs at the first cycle. Fatigue may occur at stresses less than the yield stress, and the number of cycles to failure has been related to this fatigue stress. Additional criteria give the number of cycles related to the dissipated energy needed to bring the material to melting or to a threshold of the strain energy. In all criteria considered, the number of cycles to failure results inversely proportional to the amplitude and to the frequency of the applied strain. The behavior of the model agrees with the experimental data.

A further refinement of the theory will involve the use of the generalized Zener model (the Cole–Cole model), the possibility of describing cyclic softening, and the use of other input strains, such as a sinusoidal strain function.

References

Bagley RI, Torvik PJ (1986) On the fractional calculus model of viscoelastic behaviour. J Rheol 30:133–155

Biancolini ME, Brutti C, Paparo G, Zanini A (2006) Fatigue cracks nucleation on steel, acoustic emission and fractal analysis. Int J Fatigue 28:1820–1825

Caputo M (1967) Linear model of dissipation whose Q is almost frequency independent-II. Geophys J R Astron Soc 13:529–539

Caputo M (1979) A model for the fatigue in elastic materials with frequency independent Q. J Acoust Soc Am 66:176–179

Caputo M (1995a) Distance measurements, splitting of electromagnetic waves caused by the dispersion and GPS retrieval of the model atmosphere. Rend Fis Acc Naz Lincei 9:19–36

Caputo M (1995b) Distance measurements and splitting of electromagnetic waves in water caused by dispersion. Rend Fis Accad Naz Lincei 9:103–113

Caputo M, Mainardi F (1971) A new dissipation model based on memory mechanism. Pure Appl Geophys 91:134–147

Caputo M, Plastino W (1998) Rigorous time domain responses of polarizable media. Ann Geofis 41:399407

Carcione JM (2007) Wave fields in real media. Theory and numerical simulation of wave propagation in anisotropic, anelastic, porous and electromagnetic media, 2nd edition, revised and extended. Elsevier, Amsterdam

Carcione JM (2009) Theory and modeling of constant-Q P- and S-waves using fractional time derivatives. Geophysics 74:T1–T11

Carcione JM, Cavallini F, Mainardi F, Hanyga A (2002) Time-domain seismic modeling of constant Q-wave propagation using fractional derivatives. Pure Appl Geophys 159:1719–1736

Carcione JM, Poletto F, Gei D (2004) 3-D wave simulation in anelastic media using the Kelvin–Voigt constitutive equation. J Comput Phys 196:282–297

Carpick RW, Ogletree DF, Salmeron B (1997) Lateral stiffness: a new nanomechanical measurement for the determination of shear strengths with friction force microscopy. Appl Phys Lett 70(12):1548–1550

Cisotti U (1911) L'ereditarietà lineare e i fenomeni dispersivi. Il Nuovo Cimento 2(1):234–244

Cole KS, Cole RH (1941) Dispersion and absorption in dielectrics. J Chem Phys 9:341–349

Craiem D, Armentano RL (2007) A fractional derivative model to describe arterial viscoelasticity. Biorheology 44:251–263

Diethelm K (2010) The analysis of fractional differential equations: an application-oriented, exposition using differential

operators of Caputo type. In: Lecture notes in mathematics. Springer, Heidelberg
Ellyin F (1996) Fatigue damage, crack growth, and life prediction. Chapman & Hall, London
Graffi D (1928) Sulla teoria delle oscillazioni elastiche con ereditarietà. Il Nuovo Cimento 5:310–317
Jacquelin J (1991) A number of models for CPA impedances of conductors and for relaxation in non-Debye dielectrics. J Non-Cryst Solids 131:1080–1083
Körnig H, Müller G (1989) Rheological model and interpretation of postglacial uplift. Geophys J R Astron Soc 98:245–253
Heaviside O (1894) Electromagnetic theory, vol 1. The Electrician Printing and Publishing Co., London
Lee YL, Hathaway RB, Pan J, Barkey ME (2004) Fatigue testing and analysis. Theory and practice. Elsevier, Amsterdam
Liu, JY, Ross, RJ (1996) Energy criterion for fatigue strength of wood structural members. J Eng Mater Technol 118:375–378
Mainardi F (2010) Fractional calculus and waves in linear viscoelasticity: an introduction to mathematical models. World Scientific, Singapore
Mainardi F, Pagnini G (2003) The Wright functions as solutions of the time-fractional diffusion equations. Appl Math Comput 141:51–66
Makris N (1997) Three-dimensional constitutive viscoelastic laws with fractional order time derivatives. J Rheol 41(5):1007–1020
Nicolle S, Vezin P, Palierne JF (2010) A strain-hardening bi-power law for the nonlinear behaviour of biological soft tissues. J Biomech 43:927–932
Podlubny I (1999) Fractional differential equations. Academic, New York
Rao KB, Kalluri S, Halford GR, McGaw MA (1995) Serrated flow and deformation substructure at room temperature in INCONEL 718 superalloy during strain controlled fatigue. Scr Metall Mater 32(4):4938
Sugimoto T, Sasaki Y (2008) Fatigue of structural plywood under cyclic shear through thickness III: energy dissipation performance. J Wood Sci 54:169–173
Tao G, Xia Z (2008) Fatigue behavior of an epoxy polymer subjected to cyclic shear loading. Mater Sci Eng: A 486: 38–44
Weiss CJ, Everett, ME (2007) Anomalous diffusion of electromagnetic eddy currents in geological formations. J Geophys Res 112:B08102. doi:10.1029/2006JB004475
Wyss W (1986) The fractional diffusion equation. J Math Phys 27:2782–2785
Yoshida S, Kanazawa K, Yamaguchi K, Sato M, Kobayashi K, Suzuki, N (2001) Elevated-temperature fatigue properties of engineering materials. Part II. Trans Nat Res Inst Metals 20:60–83
Zhuang WZ, Halford GR (2001) Investigation of residual stress relaxation under cyclic load. Int J Fatigue 23:S31S37